MISSOURI S&T

Missouri University of Science and Technology

Scholars' Mine

International Specialty Conference on Cold-Formed Steel Structures

(2008) - 19th International Specialty Conference on Cold-Formed Steel Structures

Oct 14th, 12:00 AM

Finite Element Analytical Investigation of Torsional Bracing Requirements for Cold-formed Steel C-shaped Studs

Jennifer Tovar

Todd Helwig

Thomas Sputo

Follow this and additional works at: https://scholarsmine.mst.edu/isccss

Part of the Structural Engineering Commons

Finite Element Analytical Investigation of Torsional Bracing Requirements for Cold-Formed Steel C-Shaped Studs

Jennifer Tovar[1], Todd Helwig[2], and Thomas Sputo[3]

Abstract

This paper provides an overview of an investigation on the torsional bracing behavior of C-shaped cold-formed steel studs. Typical bracing details for the C-shaped studs consist of a steel channel that restrains twist of the cross section. Three-dimensional finite element models were used to investigate the stiffness behavior for stability braces used to improve the torsional buckling performance of the studs. The lipped C-shaped section was modeled with pin-ended boundary conditions for the stud. Multiple models of the torsional brace were evaluated including a shell element model of a bracing channel as well as several "simpler" spring configurations. The development of these models and appropriate modeling techniques for bracing is discussed in detail. Difficulties in capturing the distortional behavior in the thin walled stud are discussed. Results from eigenvalue buckling solutions are presented. Recommendations are made for extending the use of these models to a broader range of stud sizes and analysis types to obtain recommendations for torsional bracing requirements of typical cold-formed wall studs.

[1] Structural Engineer, Schwab Structural Engineering, Inc., 555 IH 35 South, Suite 230, New Braunfels, TX 78130
[2] Assistant Professor, Department of Civil, Architectural and Environmental Engineering, The University of Texas at Austin, 1 University Station C1748, Austin, TX 78712-0273
[3] Senior Lecturer, Department of Civil and Coastal Engineering, 365 Weil Hall, University of Florida, Gainesville, FL 32611 (email: sputo@ufl.edu)

Introduction

The capacity of cold-formed lipped-cee studs can be controlled by either global or local buckling modes. The possible modes consist of flexural, torsional, and torsional-flexural global modes as well as local and distortional buckling effects. Discrete bracing is often utilized to improve the global buckling behavior, and therefore increase the overall stud capacity. Discrete bracing recommendations have been provided for hot-rolled structural steel through the American Institute of Steel Construction (AISC) *Specification* since 1999. A summary of the developmental work for the AISC *Specification* (2005) provisions are provided in Yura (1995). Although the AISC Specification does not provide torsional bracing recommendations for columns, the basic requirements were developed and discussed by Helwig and Yura (1999). The basic principals from these previous studies have direct applications for cold-formed structures, however the thin-walled nature of these shapes increase the potential problems with distortion.

Cold-formed steel member bracing techniques have been utilized in construction practice through manufacturer specific recommendations and details, however no specific bracing requirements were provided for in American Iron and Steel Institute (AISI) *Specification* editions though 2004. Recent recommendations by Sputo and Beery (2006) for bracing of the flexural mode of buckling are included in the current AISI *Specification (2007)*, however torsional bracing requirements have yet to be determined.

The objective of this research project was to continue the investigation of torsional bracing requirements for axially loaded lipped, cee-shaped, cold-formed wall studs using finite element analyses. This investigation was performed through (1) building a finite element model of a single, pin ended cold-formed steel stud that is loaded in axial compression; (2) determining an appropriate method of modeling a brace to resist torsion (in addition to weak-axis flexure) at the mid-height of the stud; and (3) evaluating the torsionally braced stud model analyses and results. The bracing of thin-walled members can pose a difficult problem due to local distortions on the cross-section. Several modifications of the FEA models were considered to capture an accurate model of the actual system, while also trying to keep the system computationally economical.

Wall studs are often braced using a horizontal cold-rolled channel (CRC) attached to the stud web at mid-height. Figure 1 hows a typical bracing detail used in practice which employs an unlipped channel section with a 1.5 inch deep web, 0.5 inch flanges, and 0.054 inch thickness. Braced models tested in this

study did not include the stud perforation or clip angle shown in Figure 1. While there are a number of different connection methods, those used in this study are probably most similar to the Direct Welded (DW) connection discussed in Green, Sputo, and Urala (2004) and Sputo and Beery (2006).

Analytical Investigation

The three dimensional finite element program ANSYS (2005) was used to conduct the parametrical studies in this investigation. A series of single, unbraced lipped cee studs were modeled first to determine the appropriate application of boundary conditions and loading. Studs were modeled with web heights of 3.62 and 6 inches, flange widths of 1.62 and 2.50 inches, and thicknesses ranging from 0.043 to 0.097 inches. Simplified cross-sections with square corners, rather than rounded corners were used. All studs were modeled with a tensile modulus of elasticity (E) of 29500 ksi and Poisson's ratio (μ) of 0.3. An 8-node shell element (SHELL93 from ANSYS) was used. Pin-ended boundary conditions were simulated at the top and bottom of the stud. This was achieved by restraining the three translational degrees of freedom at a single node in each of the flanges at the bottom of the stud. At the top of the stud, the translational degrees of freedom were restrained within the plane of the stud, but longitudinal translation was allowed. A unit load of 1 kip was distributed to the nodes at the top of the channel. To reduce the localized failures due to very high web-height to thickness ratios , the member thickness at the first row of elements (on the top and bottom of the stud) was doubled for sections with a thickness less than 0.068 inches. This adjustment was intended to reflect a more realistic distribution of load to the cross-section that would usually be achieved by loading through a track channel at the top and bottom of the wall. Buckling load predictions and mode shapes for the single unbraced stud were compared to results from a previous study (Tovar 2004) for verification.

Studs were then modeled with a discrete torsional brace at midheight. The torsional brace was modeled using a shell element representation of the CRC brace (shown in Figure 1) and a number of more simple spring configurations. The shell element model is believed to provide an accurate representation of the bracing details that are used in practice. Brace parameters were tested on a stud section that had a web height of 3.62 inches, flange width of 1.62 inches, and a lip length of 0.5 inches. Wall thicknesses of 0.043 and 0.054 inches were considered. The section with a member thickness of 0.043 inches was expected to exhibit an unbraced torsional-flexural mode of buckling and local buckling when braced at the mid-height. The section with a member thickness of 0.054 inches was expected to exhibit an unbraced torsional-flexural mode of buckling (first mode) as well as torsion flexural buckling (second mode) when braced at

the mid-height (Tovar 2004). Modeling techniques used to simulate a torsional brace and a comparison of model results for two different stud sizes are provided.

The results from these eigenvalue analyses were evaluated by relating the normalized critical buckling load to the applied brace stiffness. The normalized critical buckling load is calculated by the following relationship

$$P_{cr\_normilized} = \frac{P_{cr\_braced}}{P_{cr\_unbraced}}$$ (Eq. 1)

Where $P_{cr\_normilized}$ is the normalized critical buckling load; $P_{cr\_unbraced}$ is the critical buckling load from the unbraced stud model; and P_{cr_braced} is the critical buckling load from the braced stud model. Critical buckling loads were determined from the various braced stud model analyses. Braced stud models were used to analyze a range of brace stiffness values and therefore P_{cr_braced} does not always correspond to a fully (or even partially) braced stud, but rather the critical buckling load prediction from the braced model analyses. Brace stiffness values correspond to the total stiffness provided by the brace type being modeled (units in kip-inches/rad).

The following notation is used to describe displacement and restraint in this paper (global directions). UX represents translations in the weak-axis direction of the stud (as well as axial deflections of the CRC brace). UY represents axial deflections in the stud and weak axis deflections in the CRC brace. UZ represents translations in the strong axis direction of the stud and brace.

Shell Element Modeled Torsional Brace

The first braced stud model used in this study modeled the CRC bracing member (Figure 1) using shell elements. This model is probably the most accurate representation of the bracing details that are used in practice since the stiffening effects of the stud web are captured. The web of the horizontal brace was positioned at mid-height of the stud. The near end of the brace was "connected" so that it would resist twist at the mid-height of the stud through sets of coupled nodes. All four corners of the shell element brace had UX movement coupled to adjacent nodes on the stud web (Figure 2). This ensured that any twisting of the stud at mid-height would impose a coupled force (moment) at the end of the brace. UY and UZ movement at the center-web node at the edge of each brace end were coupled to the adjacent node at mid-height of the stud. This coupling provided pinned boundary conditions at the brace ends

without resisting any strong axis lateral deformations or axial shortening of the stud.

The stiffness of a member that is pinned at one end, with a moment connection to the main member at the other end is given as:

$$\beta = \frac{3E_b I_b}{L_b} \qquad \text{(Eq. 2)}$$

Where β is the member stiffness; E_b is the modulus of elasticity of the brace material; I_b is the moment of inertia of the brace about the axis of bending; and L_b is the length of the brace. The stiffness for the shell element braced model results was initially varied by changing the length, L, of the CRC brace member and holding constant values of E (29500 ksi) and I. To capture a range of brace stiffnesses that corresponded to unbraced (and transitional) stud buckling behavior, extremely long brace lengths were required. The resulting braces were unrealistically slender and susceptible to both bending and buckling (unless specifically controlled through coupling). These models also became computationally impractical (ie. brace lengths of 3,000 to 30,000 inches required for 362S162-43). E of the brace was therefore reduced by a factor of 10 to achieve a more reasonable range of brace lengths. For the studs considered in this study, channel brace lengths that were in a more practical length range than noted above provided full torsional bracing to the stud.

To ensure the brace would remain flat as it underwent deflections in the out-of-plane (UZ) direction, UY movements were coupled for all nodes at the intersection of the brace web and each flange back to a single point (along this intersection). Weak axis brace bending as well as warping (singly-symmetric CRC sections would naturally bend with a combination of torsion and stong-axis flexure) were restrained by coupling. This ensured a pure, strong axis bending of the brace to determine the torsional stiffness.

To investigate torsional buckling behavior in the stud, it was necessary to restrain weak axis flexural buckling of the full height stud. This required a UX lateral pin at midheight of the stud. If this pin was applied at the far end of the bracing channel (similar to constructed conditions), an axial force was transferred into the brace as local or longwave buckling began to develop in the stud. For the slender braces used in this study a slight axial load in the brace resulted in significant degradation of bending stiffness of the bracing channel. In some situations buckling of the bracing channel was the lowest eigenvalue for the system.

Analysis Results

The 362S164-54 stud exhibited a single mode of torsional flexural buckling at brace stiffness values ranging from 0.17 to 2.86 kip-inches/rad. Figure 3 illustrates a typical buckled shape for this mode. The corresponding critical buckling load predictions reflect effectively unbraced behavior at the low end of these stiffness values, where the normalized capacity ratios begin at approximately 1.3. As the brace stiffness values increased, the buckling load predictions increased to as much as 3.36 times the unbraced stud predictions for a stiffness value of 2.86.

From stiffness values of 3.07 to 3.90, the stud transition to a higher buckling mode was marked by notable asymmetry in the torsional buckling shape. This transition continued to a more distinguishable second mode of torsional flexural buckling (partially braced behavior) that was distinguished beginning at a stiffness value of 4.29 and a normalized critical buckling value of 3.40 (Figure 4). As stiffness values increased, the torsional-flexural buckling response was "capped" by a close local buckling response exhibited from stiffness values of 5.37 and higher (Figure 5). The corresponding buckling load predictions were 3.42 times the unbraced stud capacity.

The 362S164-43 stud exhibited a single mode of torsional flexural buckling at brace stiffness values beginning at 0.17 and continuing through to 1.19 kip-inches/rad. Respective normalized critical buckling load predictions ranged from 1.39 to 4.44. The effective braced behavior for this stud was limited by local buckling at a stiffness value of 1.23. The corresponding critical buckling load predictions were only 2.45 times the predictions for the unbraced stud.

Spring Models for Torsional Brace

In addition to the shell element model of the CRC bracing member, three simplified brace models were used consisting of 1) a single spring model that was attached to a single node on the stud web, 2) a multiple spring model with distributed stiffness, and 3) a single spring model that was coupled to multiple nodes. The spring element models provide a relatively simple method of modeling the torsional brace when compared to the shell element model discussed above. However, several analyses were necessary to ensure that the spring element models provided reasonable reflections of the effects of cross-sectional distortion on the bracing behavior. All three spring brace models utilized the ANSYS spring element COMBIN14, which has a single rotational DOF along the axis of the spring element. These models provided an efficient method of capturing the stud buckling response over a wide range of stiffness

values, and therefore provided valuable buckling estimates and general stiffness boundaries for the relatively time consuming shell element brace models.

The single spring brace model consisted of a spring attached to a node in the center of the stud web at mid-height (See Figure 6). The spring element is a single unit (1 inch) long and oriented so that its length runs parallel to the height of the stud. This spring orientation aligns the DOF w/ the axis for torsional rotation of the cross-section. However, it is located in line with the stud web rather than with the shear center of the section. Rotation about the Y-axis (ROTY) was restrained at the other end of the spring to engage the spring stiffness for torsional stud deformations corresponding to the rotational DOF of the spring. Rotation about the X-axis (ROTX) was also restrained to prevent "pivots" at this location, but no forces are calculated for this or other DOF's.

Since the actual connections between the brace and the stud occur over a portion of the web depth in the stud, the distributed spring brace model spread the total brace stiffness over a larger portion of the stud web than idealized by the first single spring model. This model utilized a series of springs attached to nodes on the back of the stud web at mid-height (See Figure 7). Five springs were located at nodes that match the width of a typical CRC bracing member (1.5 inches). The total input stiffness was divided by the number of springs and applied accordingly. The orientation and boundary conditions were as described for the single spring model, except that rotation about the Z-axis (ROTZ) was also required to restrain additional "pivots" at these locations during analysis.

The actual connection between the bracing channel and the stud web is usually made at the flanges of the bracing channel and can be made with either welding or mechanical fasteners. It was not clear whether the distributed spring model appropriately captured the stiffening effect so another model was considered in which an attempt was made to model the stud web that overlapped the brace with an infinite stiffness. To simulate the stiffening that occurs due to the connection, the nodes at the four flange "corner" locations were coupled to a node at one end of as single spring (similar to Figure 6). Since this spring was not directly attached to the stud (and therefore not subject to UX, UY displacements of the stud) ROTY restraint was the only boundary condition required at the opposite end of the coupled spring.

Observations and Comparison of Results

Web Distortions

Localized web distortions at the brace connection were observed to influence the results for all these analyses. The high web slenderness ratios for these sections did not effectively distribute the bracing restraint to the overall cross-section of the stud. Since bracing systems follow the classic equations for springs in series, cross-sectional distortion can often render the bracing system ineffective as evidenced by the equation:

$$\frac{1}{\beta_{sys}} = \frac{1}{\beta_{brace}} + \frac{1}{\beta_{sec}}$$ (Eq. 3)

Where β_{sys} is the stiffness of the bracing system, β_{brace} is the stiffness of the brace, and β_{sec} is the stiffness of the cross-section. The stiffness of the cross-section reflects the effect of cross-sectional distortion on the system. The system stiffness in Equation 3 must be less than the smallest of the brace stiffness or the cross-sectional stiffness term.

It is important to note that displacements from eigenvalue buckling analysis do not represent specific magnitudes, but are relative to a maximum eigenvector displacement of 1.0. To compare web distortions (and buckled shapes) between the spring and shell element braced models the eigenvector deformations in the stud nodes of the shell element model should be scaled to produce comparable magnitudes. The scale factor can be obtained by dividing the translational deformation of a given node by the deformation of the node that had the largest translational deformation. For example, if the maximum stud deformation occurred at a node at the tip of the flange and had a value of 0.09, each nodal deformation was modified by UY/0.09 or UX/0.09.

Local Buckling

This study was primarily concerned with the restraint of global modes of buckling. However, in certain analyses local buckling may limit the stud capacity before a higher mode of global buckling is reached. Local buckling was observed to control some analyses due to the boundary conditions and coupling connections of the brace. When the local buckling limit was near (slightly higher) the second mode of flexural buckling it was often difficult to achieve convergence to the second mode of flexural buckling. Additionally, multiple local buckling modes often occur within a narrow range of eigenvalues. The stud results for a range of brace stiffness values therefore exhibited some variability in the critical buckling loads and mode patterns associated with this limit state.

When local buckling started to develop in the stud modeled with the shell element CRC brace, the brace coupling and attachment may have provided an unintended restraint in the development of local buckling in the stud. When local buckling starts to occur, rotation in the stud web at this location is restrained (due to UY coupling along the length of the brace) making it necessary for the buckling wave "peak" to occur at the attachment (Figure 5). This may have resulted in critical buckling results that were slightly above or below the theoretical values. The local buckling wave "peak" at the brace location also allowed some long-wave flexural deflection that was often observed in conjunction with the more symmetrical response of local buckling.

Spring Braced Models

Results for the shell element CRC braced model and all three spring braced models are plotted in Figures 8 and 9 (for studs 362S162-54 and 363S162-43 respectively). Due to excessive web distortion, the single spring model did not provide enough system stiffness to achieve a second mode buckling response in the stud. Web distortion is sensitive to the length of unrestrained portion of the web. Since this model was only connected to a single node on the stud web significant web distortion resulted in inadequate system stiffnes as was discussed in the presentation of Eq. 3. The single spring model results were limited at approximately 68 percent of the second mode response for the stud that buckled in torsional flexure (362S162-54) and approximately 81 percent for the stud that displayed local buckling (362S162-43).

The distributed spring model and coupled spring model both dramatically reduced the limiting effects of web distortion and results for these models achieved the expected braced stud buckling response. Overall buckling behavior for each of these spring braced models was comparable to the shell element braced model and useful for efficient determination of stud buckling behavior over a large range of stiffness values. Due to slight differences in brace attachment some localized differences were observed. The shell element model was limited with a braced local buckling mode where the spring models maintained the expected braced torsional-flexural mode of buckling. The normalized critical bucking loads for effectively braced behavior in the shell element model are approximately 1 percent less (for both stud sizes) than that of the spring models, providing the lower bound of braced (or second mode) buckling behavior for all three models.

For the range of stiffness values corresponding to unbraced stud buckling behavior and transitional stud buckling behavior, the spring element models

become nonlinear at lower load levels compared to the shell element brace model curves. This results in the achievement of effectively braced behavior at a slightly lower stiffness value than that of the distributed or coupled spring models. There was a difference in the rate at which the distributed spring model and the coupled spring model reached the effectively braced stud buckling behavior. This difference was extenuated in the 362S162-54 stud results due to a more gradual change in slope at the transition to a second mode for torsional flexural buckling (slope change for the local buckling limit of the 362S162-43 stud is more abrupt).

The observed cross-sectional rotations (Figure 10) indicate the shell element model provided the greatest torsional restraint as the results approached effectively braced stud buckling behavior. The distributed spring model allowed slightly more rotation and the coupled spring model allowed the most rotation. The coupled spring model exhibited single mode of torsional flexural buckling with a maximum UZ displacement occurring at 15.6 inches below the stud mid-height. The distributed spring model exhibited a more asymmetric single mode that transitioned to the second mode of torsional flexure, with a maximum UZ displacement occurring at 21.6 inches below mid-height. The shell element model, however displayed a somewhat asymmetric second mode of torsional flexure, with a maximum UZ deflection occurring at 23.4 inches below mid-height. This response approaches fully braced behavior where a perfectly symmetric buckled shape would contain maximum twist at the L/4 or 24 inches above and below mid-height. A closer look the web distortions (Figure 11) showed similar curvature and distortion (although inverted) at the points of attachment for the coupled spring and shell element models. Due to the differences in node connectivity the distributed spring maintains relatively linear web distortions at brace attachment. However, the shell element braced model restrained overall cross-section rotations slightly better than either of the two spring braced models and is probably the most accurate representation of the problem compared to details used in practice.

One final observation from all three spring model types was that critical buckling load predictions for braced models were always higher than lipped cee stud predictions (with no brace attached). Spring models were analyzed at a stiffness value of 0.0, however normalized critical buckling loads show that predictions for both studs were approximately 1.14 times higher than model predictions when no brace applied. A small portion (about 4 percent) of this difference was attributed to small changes in the stud mesh that provided the node locations necessary for brace attachment. The majority (remaining 10 percent) of this difference was thought to be due to the pin that was applied to resist weak axis lateral deflection in the braced stud models. This restraint

forces the stud section to twist about the pin, which is located on the stud web, rather than about the section shear center.

Summary and Conclusions

A number of finite element modeling techniques were used in this study to investigate the torsional bracing requirements for cold-formed lipped-cee wall studs. Eigenvalue buckling analyses were performed for two pin-ended studs (362S162-43 and 362S162-54) that were loaded in compression and braced at mid-height. Brace stiffness was applied through a shell element model of the bracing channel member, a single spring, a series of springs distributed along the web location of the bracing channel, and single spring coupled at the corner locations of the bracing channel flanges. Analyses were performed for a range of brace stiffness values to determine the stiffness range required to achieve braced stud behavior.

The shell element bracing model is believed to be the most accurate representation of details that are used in practice, but it is time consuming and suseptable to controlling local buckling effects. The spring models provide simple methods of simulating the bracing behavior; but some difference in the effects of cross-sectional distortion was observed. Overall bracing behavior and normalized critical buckling loads showed that the distributed spring and coupled spring models had reasonable agreement with the shell element braced model. All three models produced results that were close to CUFSM critical buckling predictions for braced and unbraced stud behavior (Tovar 2004).

It is recommended that a spring braced model be utilized to analyze bracing behavior of a broader range of lipped-cee stud sizes. Based on results and observations from this study the following conclusions and recommendations are provided for extending this work:

1) Critical buckling load predictions and mode shapes have been shown to be sensitive to specific details of CRC brace attachment to the stud, particularly in the shell element brace model.
2) Appropriate spring braced models provide an efficient, less sensitive alternative to obtaining results for the general range of stiffness values that correspond to the transition between unbraced buckling and braced buckling behavior for the stud.
3) The shell element braced model could be used to "spot check," or make comparisons at a few stiffness values of interest, based on overall critical buckling curves developed using a spring braced model.

4) Critical buckling load predictions and mode shapes from analyses when stiffness values are equal to zero and when they provide effectively braced stud behavior should be compared to expected results from an outside source to ensure convergence on the correct mode.

5) Results from modeling of the lipped-cee stud in this study showed good comparison for a range of stud sizes with web heights of 3.62 and 6 inch, flange widths of 1.62 inches, and member thicknesses from 0.033 to 0.097 inches. The use of these models for greater web-height-to-thickness or flange-width-to-thickness ratios may require model adjustments to avoid localized effects of loading and boundary conditions.

Future Work

With consideration for the recommendations given above, these bracing models could be applied to a broader range of typical stud sizes to determine general torsional stiffness requirements for a single lipped-cee wall stud. Additional extensions could be made to obtain torsional brace strength requirements by performing a large displacement analysis. The ANSYS command files used in this study along with more detailed information about model development can be found in Tovar 2007.
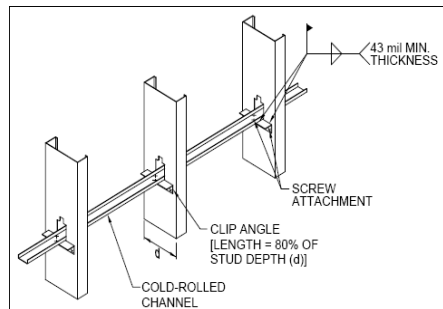
Figure 1. SSMA Channel Bracing Detail (SSMA, Cold-Formed Steel Details)
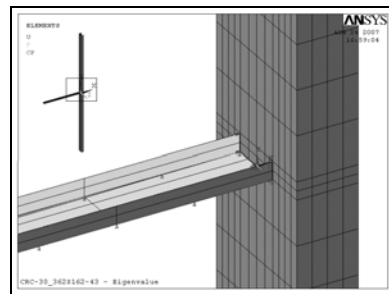
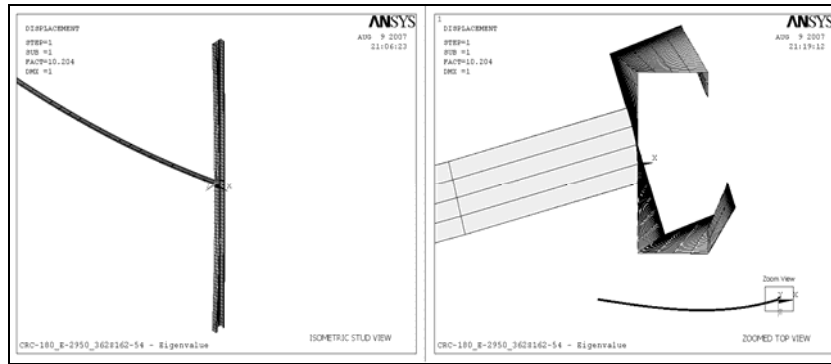**Figure 2.** Shell Element Braced Model (ANSYS, Inc. v.10.0)

Figure 3. Unbraced Torsional-Flexural Buckling of 362S162-54 Stud
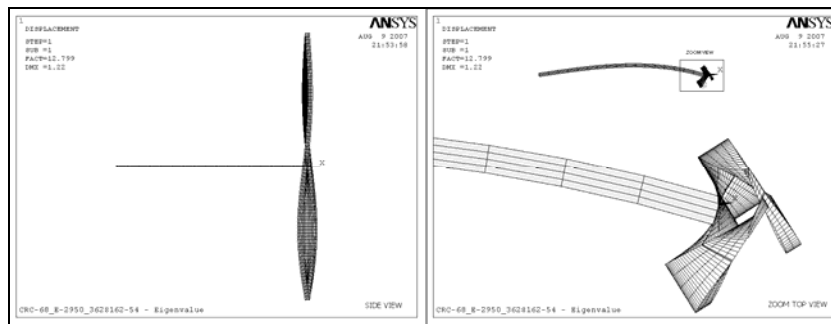

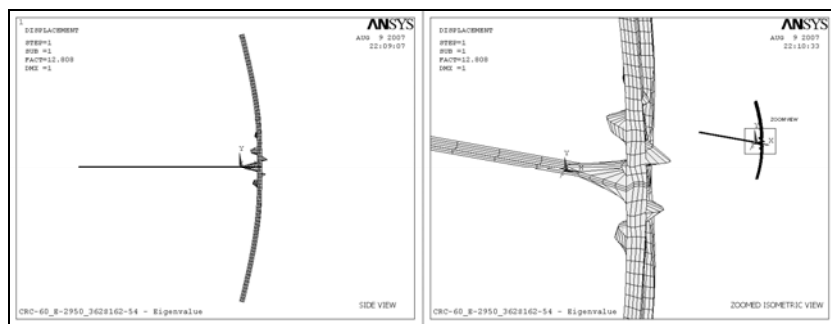**Figure 4.** Partially Braced Second ModeTorsional-Flexural Buckling of 362S162-54 Stud
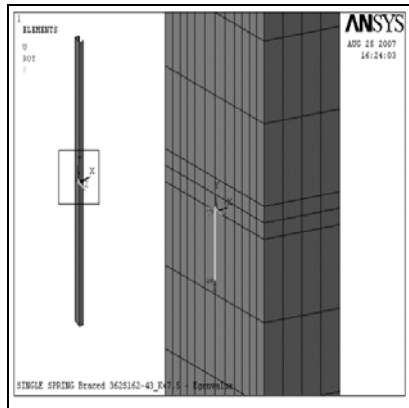

Figure 5. Braced Local Buckling of 362S162-54 Stud
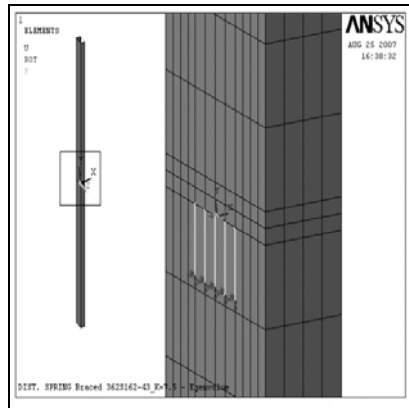
Figure 6. Single Spring Braced Model (ANSYS, Inc. v.10.0)

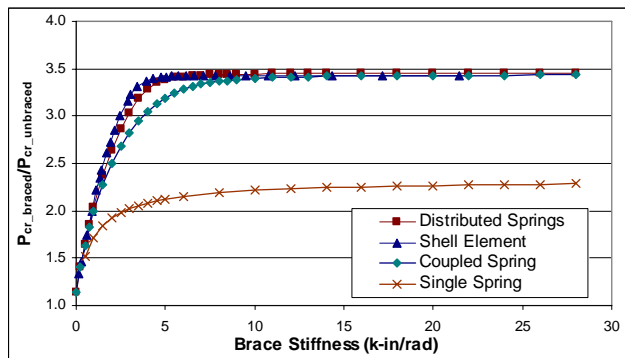**Figure 7.** Distributed Spring Braced Model (ANSYS, Inc. v.10.0)

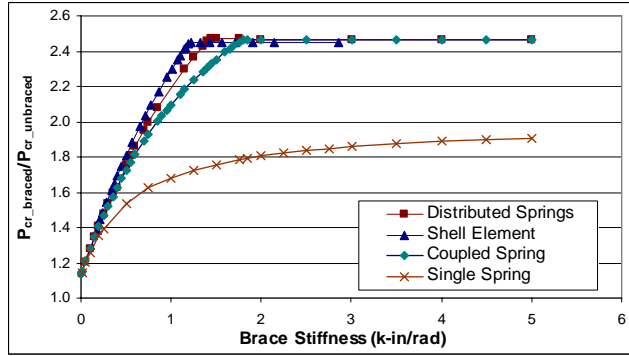**Figure 8.** Web Brace Model Comparison for the 362S162-54 Stud

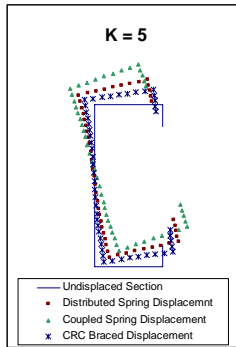**Figure 9.** Brace Model Comparison for the 362S162-43 Stud

Figure 10. Cross-section of Braced Models for the 362S162-54 Stud
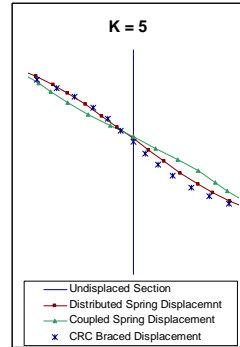

Figure 11. Web Distorion of Braced Models for the 362S162-54 Stud

Appendix. – References

ANSYS. (2005) Version 10.0. SAS IP, Inc.

American Institute of Steel Construction (AISC) (2005). *Specification for Structural Steel Buildings*, American Institute of Steel Construction, Chicago, IL.

American Iron and Steel Institute (AISI) (2007). *North American Specification for the Design of Cold-Formed Steel Structural Members and Commentary*, Washington DC.

CUFSM. (2004) Version 2.6.

Green, P.S., Sputo, T. and Urala, V. (2004). "Bracing Strength and Stiffness Requirements for Axially Loaded Lipped Cee Studs." *Proceedings, 17th International Specialty Conference on Cold-Formed Steel*, Orlando, FL.

Helwig, T.A., Yura, J.A., (1999). "Torsional Bracing of Columns." *Journal of Structural Engineering,* Vol. 125, No. 5, p 547-555.

Sputo, T. and Beery, K. (2006). "Accumulation of Bracing Strength and Stiffness Demand in Cold-Formed Steel Stud Walls." *Proceedings, 18th International Specialty Conference on Cold-Formed Steel*, Orlando, FL.

Steel Studs Manufacturers Association (SSMA) (2001). *Cold-Formed Steel Details,* Steel Studs Manufacturers Association, Chicago, IL.

Tovar, J. (2004). "Application of the Direct Strength Method to Axially Loaded, Perforated Cold-Formed Steel Studs", Honors Thesis, University of Florida, Gainesville, FL.

Tovar, J. (2007)."Finite Element Analyitical Investigation of Torsional Bracing Requirements for Cold-Formed Steel C-Shaped Studs", M.S. Thesis, University of Texas, Austin, TX.

Yura, J.A. (1995). "Bracing for Stability – State of the Art." *Bracing for Stability,* Structural Stability Research Council, Bethlehem, PA.